*Proc. Natl. Acad. Sci. USA*
Vol. 93, pp. 9431–9436, September 1996
Biochemistry

# The mode of action and the structure of a herbicide in complex with its target: Binding of activated hydantocidin to the feedback regulation site of adenylosuccinate synthetase

R. FONNÉ-PFISTER*†, P. CHEMLA*, E. WARD‡, M. GIRARDET*, K. E. KREUZ*, R. B. HONZATKO§, H. J. FROMM§, H.-P. SCHÄR*, M. G. GRÜTTER¶, AND S. W. COWAN-JACOB†¶‖

*Research and Development, Crop Protection, and ¶Core Drug Discovery Technologies, Pharmaceutical Division, Ciba–Geigy Ltd., 4002 Basel, Switzerland; ‡Biotechnology Research Unit, Ciba–Geigy Ltd., P.O. Box 12257, Research Triangle Park, NC 27709-2257; and §Department of Biochemistry and Biophysics, Iowa State University, Ames, IA 50011

*Communicated by Brian W. Matthews, University of Oregon, Eugene, OR, May 30, 1996 (received for review April 15, 1996)*

**ABSTRACT** **(+)-Hydantocidin, a recently discovered natural spironucleoside with potent herbicidal activity, is shown to be a proherbicide that, after phosphorylation at the 5′ position, inhibits adenylosuccinate synthetase, an enzyme involved in *de novo* purine synthesis. The mode of binding of hydantocidin 5′-monophosphate to the target enzyme was analyzed by determining the crystal structure of the enzyme-inhibitor complex at 2.6-Å resolution. It was found that adenylosuccinate synthetase binds the phosphorylated compound in the same fashion as it does adenosine 5′-monophosphate, the natural feedback regulator of this enzyme. This work provides the first crystal structure of a herbicide–target complex reported to date.**

Despite nearly 60 years of herbicide research and commercial development, the known biochemical modes of herbicidal action remain few (1). Motivation to find new sites of action comes not just from curiosity about plant biochemistry. Weed resistance to several classes of herbicides (2), as well as strict environmental and safety requirements, demand new herbicides acting with novel modes of action and make lead finding a constant challenge. Among the methods used to find new lead structures, the screening of metabolites produced by microorganisms has been proven important (3).

(+)-Hydantocidin is a naturally occurring spironucleoside isolated from *Streptomyces hygroscopicus* (4–8) that exhibits an interesting profile of growth-regulatory and herbicidal activities against monocotyledonous and dicotyledonous annual weeds, with no toxicity to microorganisms, fungi, fish, and mice (6). Its intriguing structure and remarkable biological properties have stimulated a considerable amount of synthetic work on the parent compound (9–14) and its analogues (15–25). The novel injury symptoms it elicits in plants has prompted a detailed investigation of its mode of action. We show here that adenylosuccinate synthetase (AdSS), an essential enzyme for *de novo* AMP synthesis (see Fig. 1*a*), is the herbicide target site and that hydantocidin is phosphorylated to form the active principle hydantocidin 5′-monophosphate (HMP). X-ray analysis of the complexes AdSS–HMP and AdSS–AMP shows that AdSS binds HMP in the same way that it binds AMP, the natural feedback regulator of the enzyme (26).

## MATERIALS AND METHODS

**Basil Cell Culture.** Cells of *Ocymum basilicum* (basil) were treated as described (27). All measurements were performed in triplicate. $IC_{50}$ values of cell growth were calculated using the GRAFIT program (Erathicus Software, London, U.K.). Reversion studies were carried out in basic growth medium supplemented with 1 mM AMP. [$^{14}$C]Hydantocidin was synthesized by Ciba–Geigy (P. Ackermann, P. Thuer, and S. Mirza, personal communication).

**Enzyme Assay.** The standard assay for bacterial AdSS (28) contained (in a final volume of 50 μl): 50 mM Hepes·KOH (pH 7.4), 1 mM dithioerythritol, 2 mM Mg·acetate, 1.5 mM aspartate, 0.1–0.25 mM GTP, 0.08 mM IMP, 0.02 mM [$^{14}$C]IMP, a GTP regeneration system consisting of 4 mM phosphocreatine, 5 units of creatine phosphokinase, and 14 ng of bacterial AdSS. Similar conditions were used for the determination of AdSS from wheat germ with the exception that 3.5 mM aspartate and 10 μM GTP were used and between 0.16 μg and 50 μg of protein depending on the purification level of the enzyme. All incubations were started by the addition of protein, carried out at 35°C for 30 min, and terminated by the addition of 50 μl of 30 mM tetrabutylammonium hydrogen sulfate (TBAHS). Quantification of metabolites was based on their radioactivity distribution in HPLC profiles. HPLC was performed on a Nucleosil (Macherey–Nagel, Oesingen, Switzerland) 120 C-18 column (125 × 4 mm, particle size 3 μm) connected to an HPLC radioactivity monitor (LB 507B; Berthold, Nashua, NH). The column was eluted at 0.8 ml/min with a linear gradient from 80% buffer A (40 mM $KH_2PO_4$·KOH, pH 5.2/5 mM TBAHS)/20% buffer B (100 mM $KH_2PO_4$·KOH, pH 5.2/5 mM TBAHS) to 90% buffer B for 5 min followed by an isocratic elution for 10 min.

**Plant AdSS Purification.** AdSS extraction and purification were done using a strategy different from the one previously described (29). Acetone powder (100 g) from wheat germ was resuspended in 2850 ml of 10 mM $KH_2PO_4$·KOH, pH 7.4/1 mM dithioerythritol/1 mM EDTA (buffer C) and agitated for 20 min at 4°C. The suspension was filtered through miracloth, and the filtrate was centrifuged at 10,000 × *g* for 10 min (raw extract). The enzyme activity precipitated between 35 and 70% ammonium sulfate and was resuspended in 500 ml of 10 mM $KH_2PO_4$·KOH, pH 7.4/1 mM dithioerythritol/1 mM EDTA and desalted over a G25 Sephadex column (45 × 5 cm). The desalted protein fractions were loaded onto a 85 × 10 mm DEAE Sepharose fast protein liquid chromatography column,

The publication costs of this article were defrayed in part by page charge payment. This article must therefore be hereby marked "*advertisement*" in accordance with 18 U.S.C. §1734 solely to indicate this fact.

Abbreviations: HMP, hydantocidin 5′-monophosphate; AdSS, adenylosuccinate synthetase.

Data deposition: The sequences reported in this paper have been deposited in the GenBank data base [accession nos. U49389 (*A. thaliana*), U49388 (*Z. mays*), and U49387 (*T. aestivum*)].

Data deposition: The atomic coordinates and structure factors have been deposited in the Protein Data Bank, Biology Department, Brookhaven National Laboratory, Upton, NY 11973 (references 1SOO and R1SOOSF for AdSS in complex with HMP; references 1SON and R1SONSF for AdSS in complex with AMP; and reference 1ADE for unligated AdSS).

†R.F.-P. and S.W.C.-J. contributed equally to this work.

‖To whom reprint requests should be addressed.

which was washed with 5 volumes of buffer C containing 10 mM NaCl. Enzyme was eluted from this column using a linear gradient of 10–200 mM NaCl in buffer C. Fractions of 2 ml were collected, and the active ones were combined and desalted through G25 columns and applied to a Cibacron Blue 3GA column (265 × 25 mmc; Sigma). After equilibration and washing with buffer C, elution was carried out using a linear gradient of 0–4 mM GTP in buffer C. Fractions of 2 ml were collected the active fractions were pooled, washed, and concentrated to a final volume of 2 ml over an Amicon concentrator (membrane YM30) with 100 mM $KH_2PO_4$·KOH, pH 7.4/1 mM dithioerythritol/1 mM EDTA.

**Synthesis of HMP.** 2′,3′-isopropylidene hydantocidin **1** was treated with dibenzylphosphate in the presence of diethylazodicarboxylate and triphenylphosphine in tetrahydrofuran at room temperature to give the phosphodiester **2** (85% yield). Following hydrolysis of the isopropylidene protecting group in aqueous trifluoroacetic acid, hydrogenolysis of the benzyl diester gave a good yield of HMP **3** (see Fig. 2).

**Plant AdSS cDNA Sequences.** The *Arabidopsis thaliana* clone was isolated by transforming the *Escherichia coli purA* mutant strain PC 0543 (CGSC 35: *E. coli* Genetic Stock Center) with a cDNA library cloned in the expression vector pFL61 (30) and selecting for adenine prototrophs. The identity of a cDNA insert from prototrophy-conferring plasmids was confirmed by DNA sequencing with fluorescent dideoxy terminators. AdSS cDNA clones from *Zea mays* and *Triticum aestivum* were isolated by low-stringency hybridization of the labeled *A. thaliana* clone to cDNA libraries cloned in phage λ Unizap (Stratagene).

**Crystallization of AdSS–Inhibitor Complexes.** Recombinant AdSS was prepared from a genetically engineered strain of *E. coli* (28). After concentration to 19 mg/ml in a buffer containing 20 mM imidazole, 75 mM succinate, and 70 μl of 2-mercaptoethanol per liter at pH 7.7, the protein was crystallized according to Serra *et al.* (31). However, soaking of these crystals with either HMP or AMP resulted in cracking; therefore, cocrystallization was necessary. The protein was incubated with HMP at a molar ratio of 1:5 for at least 30 min then crystallized using the hanging drop method of vapor diffusion from ammonium sulfate and 30% PEG 4000 at pH 4.7. Crystals appeared after 1 day and grew to 0.4 × 0.2 × 0.2 $mm^3$ over a period of 1 week. Crystals of AdSS in complex with AMP were obtained after incubation of the enzyme with a 10-fold molar excess of the feedback inhibitor from 0.2 M sodium acetate, 0.1 M Tris·HCl, and 30% PEG 4000 at pH 8.6. These crystals are isomorphous to those obtained for the AdSS–HMP complex (space group $P4_32_12$). Data for the AdSS–HMP complex were collected from one crystal to 2.6 Å on a FAST area detector (Delft Instruments, Delft, the Netherlands) over a period of 5 days. Data for the AdSS–AMP complex were collected using a MAR image plate detector (Marresearch, Hamburg) to a resolution of 2.55 Å, also from only one crystal. The quality of the AdSS–AMP data is better, although the crystal was smaller, as the data collection took only 1 day due to the more suitable geometry of the image plate for large unit cells.

**X-Ray Structure Determinations.** The structure of the AdSS–HMP complex was determined using molecular replacement methods (32) implemented in the program suite X-PLOR (33). The structure of unligated *E. coli* AdSS (34) was used in its entirety as the search model (Protein Data Bank access code 1ADE). After rigid body refinement of the position of the monomer in the asymmetric unit, the *R* factor was 51.8% using all data to 2.6-Å resolution. Refinement continued using alternate cycles of minimization with X-PLOR (33), and model building using the program O (35). To minimize the number of variables, temperature factors were refined for groups of atoms. The AdSS–AMP structure was obtained starting with rigid body refinement of the position of AdSS from the AdSS–HMP complex in the AdSS–AMP cell. Inhibitor positions were determined unambiguously from difference Fourier maps and were included in the models when the *R* factor dropped below 23%. Final refinement statistics are listed in Table 1.

## RESULTS AND DISCUSSION

**Elucidation of the Mode of Action.** For easier handling and to avoid uptake problems, the growth of a basil (*O. basilicum*)

Table 1. X-ray data collection and refinement statistics

| | AdSS–HMP | AdSS–AMP |
|---|---|---|
| Data collection | | |
| Unit cell dimensions, Å | $a = b = 70.5$, $c = 198.8$ | $a = b = 70.5$, $c = 201.2$ |
| Resolution, Å | 2.6 | 2.55 |
| Unique reflections, no. | 15433 | 17293 |
| Completeness, % | 95.1 | 99.7 |
| Multiplicity | 2.5 | 6.7 |
| $R_{merge}$,* % | 11.0 | 8.6 |
| Refinement | | |
| *R* factor,† % (all data, Å) | 18.7 (8.0–2.6) | 18.7 (8.0–2.55) |
| Deviations from ideal geometry | | |
| Bonds, Å | 0.011 | 0.011 |
| Angles in degrees | 1.66 | 1.71 |
| Ramachandran outliers‡ | 0 | 2 (generously allowed) |
| Contents of final model | 431 amino acids | 431 amino acids |
| | 78 water molecules | 93 water molecules |
| | 1 HMP molecule | 1 AMP molecule |
| | 1 2-mercaptoethanol | 1 2-mercaptoethanol |
| | 3 sulfur ions | |
| | 1 sodium ion | |
| Average temperature factors | | |
| Main chain | 22.41 | 30.75 |
| Side chain | 33.20 | 37.83 |
| Inhibitor | 17.00 | 24.55 |

*$R_{merge} = \Sigma\Sigma_j |I_j - \langle I \rangle| / \Sigma \langle I \rangle|$, where $I_j$ is the *j*th measurement of the intensity of reflection *I*.
†*R* factor = $\Sigma || F_{obs}| - |F_{calc} || / \Sigma |F_{obs}|$.
‡Calculated using PROCHECK (36).

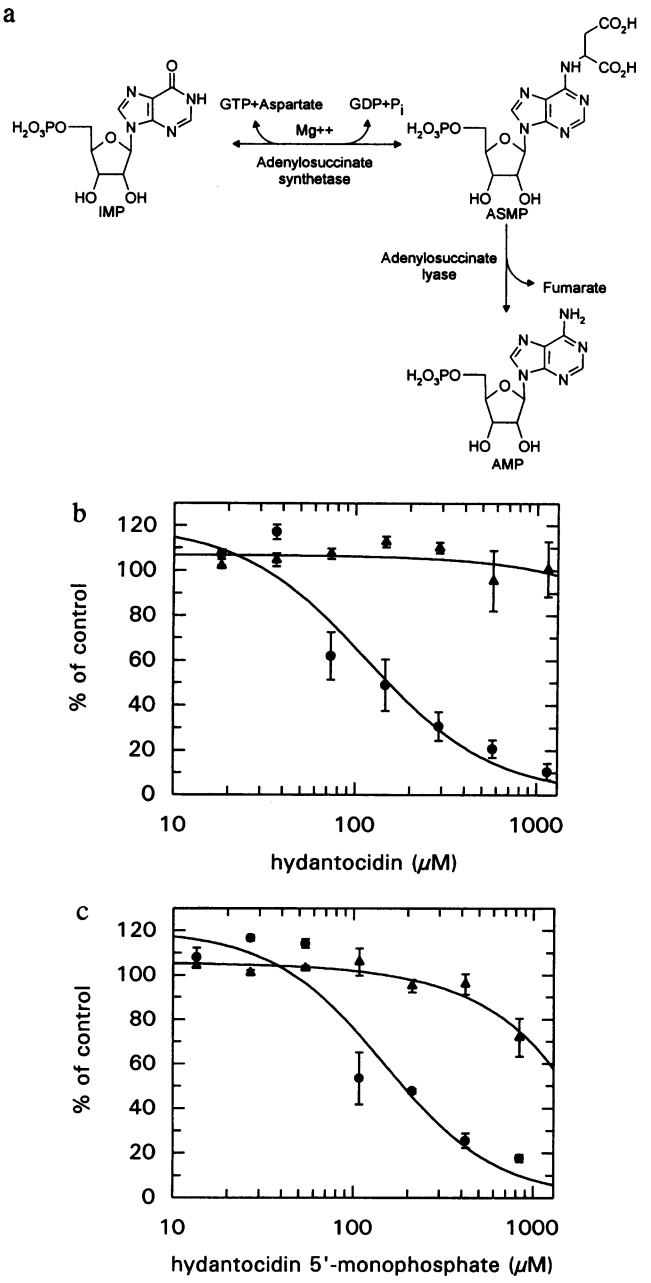


FIG. 1. (*a*) Reaction sequence leading from IMP to AMP in *de novo* purine biosynthesis. Effect of hydantocidin (*b*) and HMP (*c*) on basil cell growth in the absence or presence of AMP in the culture medium. ●, Basil cell growth in basic medium; and ▲, basil cell growth in supplemented medium.

cell suspension was used as an *in vivo* model system to replace whole plants. Hydantocidin inhibited basil cell growth ($IC_{50}$, 116 μM ± 21) (Fig. 1*b*), and this effect was not altered by the addition of a mixture of essential amino acids, pyrimidines, vitamins, and other cofactors. However, supplementation of the medium with the purine nucleotides ATP, ADP, or AMP reversed growth inhibition, the most potent compound being AMP (Fig. 1*c*). Uptake of [$^{14}$C]hydantocidin was unaffected by the presence of AMP in the culture medium (data not shown), suggesting that hydantocidin directly affects AMP biosynthesis. Since the addition of guanine, hypoxanthine, uric acid, or allantoin to the culture medium did not effect growth inhibition, hydantocidin was expected to inhibit the *de novo* AMP synthesis pathway and not purine salvage or degradation.

In addition, basil cell growth inhibition was not affected by the addition of IMP, suggesting that hydantocidin inhibits purine biosynthesis between IMP and AMP (Fig. 1*a*). This biotransformation requires two enzymatic steps. First, AdSS (EC 6.3.4.4) catalyzes the transfer of aspartate to IMP, yielding the intermediate adenylosuccinate (37). The next enzymatic step, leading to AMP with the release of fumarate, is catalyzed by adenylosuccinate lyase (EC 4.3.2.2). Adenylosuccinate is very toxic to basil cells, and consequently no reversion studies were possible with this compound. An assay using [$^{14}$C]IMP was developed to measure AdSS activity by monitoring the formation of labeled adenylosuccinate after its separation from the substrate IMP by HPLC. Furthermore, this method allowed the separation of all metabolites of the purine pathway from IMP to ATP. Yeast adenylosuccinate lyase activity was assayed as described (38, 39).

Surprisingly, neither activity was affected by hydantocidin, even at concentrations as high as 35 mM for *E. coli* AdSS and 25 mM for yeast adenylosuccinate lyase. The only potent inhibitor of AdSS that has been previously described is hadacidin, a competitive inhibitor of aspartate (40, 41). In comparison to hydantocidin, hadacidin is 8 times more potent on basil cells ($IC_{50}$, 14 μM ± 2), although in whole plants it is 20 times less active than hydantocidin. A complete reversion of cell growth inhibition by hadacidin was also observed after 1 mM AMP was added to the culture medium (Fig. 1*c*). Hadacidin thus shows similar behavior to hydantocidin in basil cells. These observations were additional arguments in favor of hydantocidin being an AdSS inhibitor, although no inhibition of purified bacterial AdSS *in vitro* with hydantocidin was detected.

The puzzling lack of activity of hydantocidin *in vitro* was investigated further. Using a crude wheat germ extract, AdSS was found to be weakly inhibited by hydantocidin. However, the degree of inhibition (typical $IC_{50}$, 830 μM ± 14) varied depending on the crude extract preparation. Furthermore, potential phosphate donors such as ATP or GTP increased the inhibition potency of hydantocidin by a factor of 7.5 in this *in vitro* system. The enzyme from wheat germ was partially purified (≈300-fold), yielding a specific activity of 260 nmol/min/mg. Surprisingly, as for the bacterial enzyme, hydantocidin did not show any significant inhibition of the partially purified plant AdSS activity, in contrast to that observed in the raw extract. On the other hand hadacidin potently inhibited both the wheat germ AdSS activity in a crude extract ($IC_{50}$, 15 μM ± 1) as well as in the enriched fractions ($IC_{50}$, 24 μM ± 1), as expected. All these results led us to suspect that hydantocidin could be a prodrug, as recently suggested (42, 43).

[$^{14}$C]Hydantocidin was then used to analyze a possible transformation of this herbicide in plants. TLC separation revealed that hydantocidin was metabolized by *A. thaliana* plantlets to a highly polar form (relative $R_f$ values of 0.56 ± 0.02 and 0.03 ± 0.01, respectively). The metabolite accounted for 28 ± 2% of the total extractable radioactivity from *A. thaliana* plantlets after 24 h. After treatment of the radioactive metabolite with an acid phosphatase, a compound with an identical $R_f$ to hydantocidin was recovered, suggesting that the metabolite was phosphorylated.

HMP was synthezised (Fig. 2) and was found to coelute with the polar metabolite based on TLC and HPLC analysis. In addition HMP proved to be a good *in vivo* inhibitor of basil suspension cell growth, with a similar potency to hydantocidin ($IC_{50}$, 148 μM ± 29; Fig. 1*c*). As for hydantocidin, the cytotoxicity of HMP was totally alleviated by supplementation of the growth medium with 1 mM AMP. Importantly, HMP was also a potent *in vitro* inhibitor of both bacterial and plant AdSS ($IC_{50}$, 86nM ± 5 and 857nM ± 36, respectively). These observations indicate that hydantocidin is activated in plant cells to yield the active herbicidal principle, which is HMP.

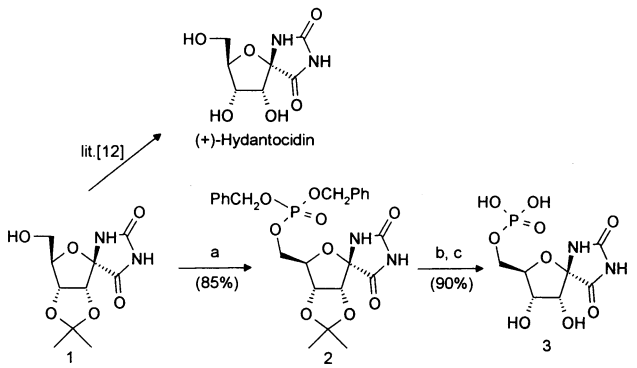


FIG. 2. Synthesis of HMP.

During preparation of this manuscript, the same finding was presented by C. Cseke *et al.***

**Similarity of Plant and Bacterial AdSS Sequences.** A cDNA encoding AdSS was isolated from *A. thaliana* by phenotypic complementation of a *purA* mutant of *E. coli*. Homologous sequences were identified and isolated from *Zea mays* and *Triticum aestivum*. Fig. 3 shows the predicted protein sequences encoded by the three plant clones, aligned with the *E. coli* sequence. The plant sequences share on average >40% identity with the bacterial sequence. In addition, the plant sequences extend beyond the *E. coli* sequence at their amino termini (data not shown). The sequence composition of these extensions indicate that they may encode chloroplast transit peptides (45) consistent with the intracellular location of the pathway (46).

It is now well accepted that protein sequences with >30% identity will have the same fold (47). Therefore, the recently determined three-dimensional structure of *E. coli* AdSS in the apo form (48) could be used as a model for the plant target of HMP. Crystals, diffracting to 2.6-Å resolution, were grown for *E. coli* AdSS in complex with HMP and also in complex with AMP (see legend to Table 1). AMP, the product of adenylosuccinate lyase, is a feedback inhibitor of AdSS and competitive with the substrate IMP (26). These structures were determined using the molecular replacement method (32) with the apo–AdSS structure (34) as a search model. A comparison of residues lining the binding site of HMP or AMP in AdSS shows that these residues are strictly conserved among the bacterial and plant AdSS sequences (Fig. 3), which lends support to the validity of the *E. coli* model of plant AdSS inhibition.

**Structure of Inhibited AdSS.** As described by Poland and colleagues (34, 48), AdSS consists of a 10-stranded, mostly parallel β-sheet surrounded by many, largely helical, crossover connections. On complexation with either HMP or AMP, the enzyme undergoes large conformational changes, closing over the active site crevice and covering the inhibitor (Fig. 4). The mean rms deviation between the uncomplexed and the inhibitor-bound structures is 2.0 Å (using all 431 Cα atoms), with the largest shifts (up to 11 Å for equivalent Cα atoms) occurring in several loops surrounding the active site crevice (Fig. 4). These same loops (residues 44–50, 121–129, and 299–302) were found to have the highest temperature factors in the apo-structures (34, 48), indicating an inherent flexibility. The conformation of two of these loops is not affected by crystal contacts in the HMP and AMP complexes, but the loop around residue 300 has some interactions with a neighboring molecule.

**Cseke, C., Grouse, G. D., Murdoch, M. G., Gerwick, B. C., Green, S. B. & Heim, D. R., Meeting of the Weed Science Society of America, Feb. 5–8, 1996, Norfolk, VA, abstr. 324.

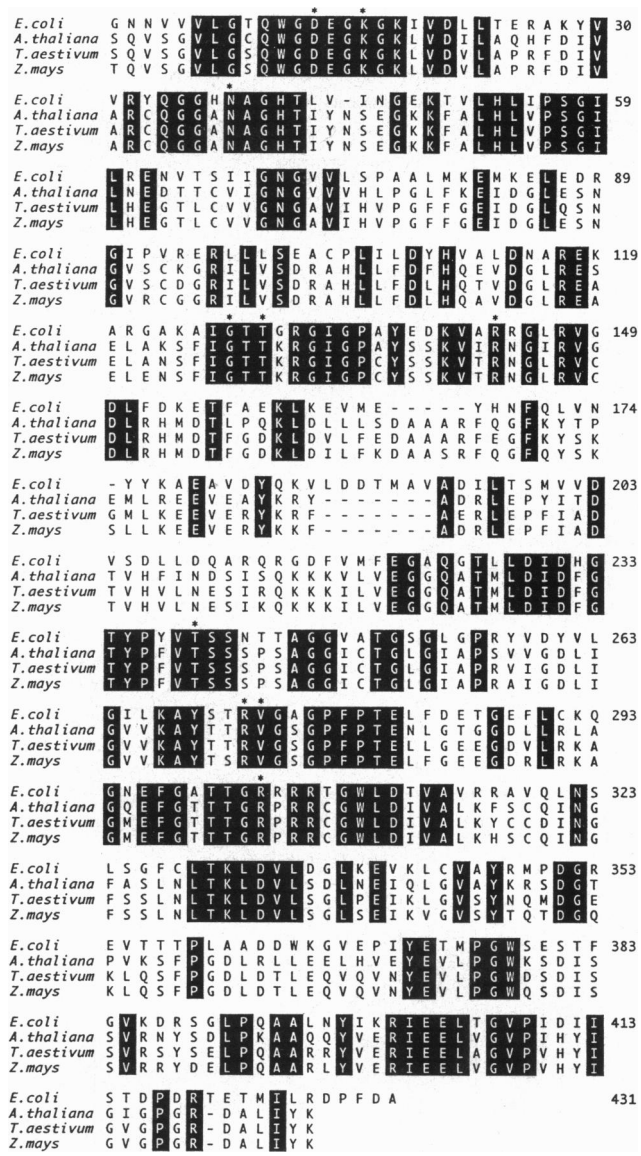


FIG. 3. An alignment of the predicted protein sequences encoded by the *E. coli* AdSS gene and AdSS cDNA clones from *A. thaliana*, *Z. mays*, and *T. aestivum*. The numbering corresponds to the sequence of the mature *E. coli* protein, which lacks the initiator methionine (44). The first residue depicted in the *A. thaliana* sequence is encoded by the 66th codon of the open reading frame; the first residue of the *Z. mays* protein is encoded by the 60th codon. The wheat clone was truncated 3′ to the predicted position of an initiator methionine codon. Amino acid residues identical among all four sequences are shaded. Residues implicated in binding HMP or AMP are marked with asterisks.

The dramatic loop movements are accompanied by shifts throughout the whole structure with the smallest differences occurring in the central β-sheet region. In fact, ligand binding at the C-terminal end of the β-sheet causes the movement of the long crossover connections between β-strands, which contain these loops.

The rms deviation between AdSS complexed with HMP and AdSS complexed with AMP is 0.35 Å for the 431 Cα atoms, which is close to the level of experimental error for structures at 2.6-Å resolution. In fact, the two inhibitors bind to the enzyme in the same site (Fig. 5) and with a very similar conformation (Fig. 4). Hence, HMP is a mimic of the feedback inhibitor AMP. The phosphate group is very important for binding to the enzyme and involves most of the direct contacts that the inhibitors have with the protein, including hydrogen

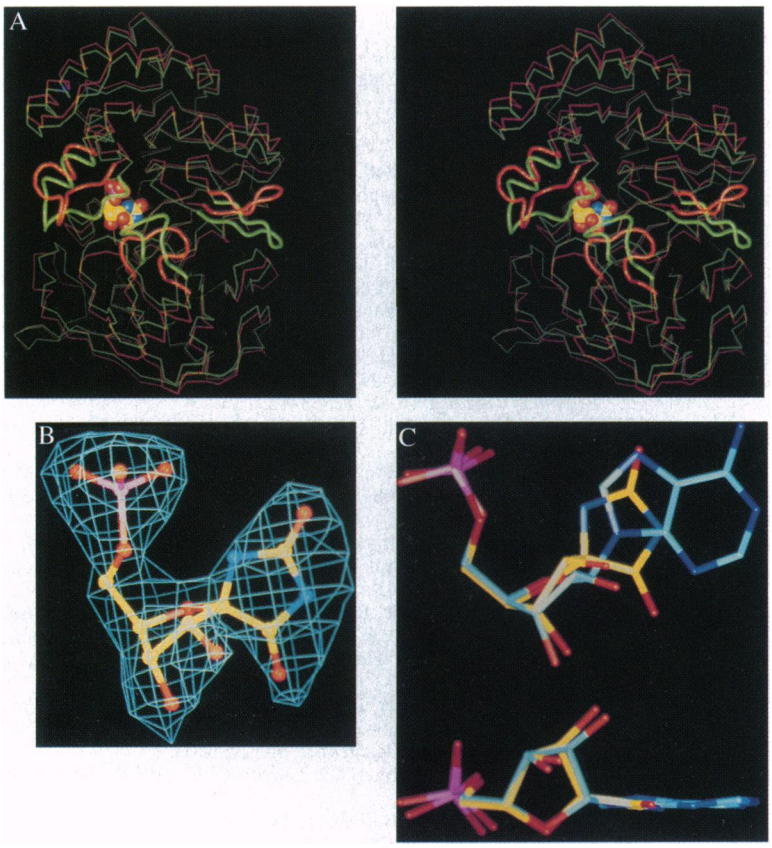


FIG. 4. (*A*) Stereoview of apo- and HMP-bound *E. coli* AdSS (the Cα traces are colored red and green, respectively). The structural alignment is based on 408 Cα atoms, which can be superimposed within 4.0 Å (rms deviation, 1.48 Å). Only one monomer is shown for clarity. The binding sites on the monomers are well separated from each other in the dimer. The three loops where the largest shifts occur are shown as smooth tubes [including residues 121–129 (*Left*), 299–302 (*Middle*), and 44–50 (*Right*). Two of these cover the HMP binding site where HMP is shown by solid spheres, while the β-hairpin to the right lies above the GTP binding site. (*B*) 2Fo-Fc Fourier map for HMP calculated by omitting HMP from the final model (contoured at 2σ). (*C*) Superposition of HMP- (yellow) and AMP- (blue) based on the coordinates of the protein Cα atoms only. The two views shown are exactly 90° apart.

bonds to Arg-143 from the other monomer in the dimer. The large shift in the loop between helices 3 and 4 allows Thr-129 to contribute to the phosphate binding. The 2′ and 3′ hydroxyl groups of the ribose moiety have hydrogen bonds with Arg-303 and the main-chain carbonyls of Gly-127 and Val-273 (Fig. 5). Although Arg-303 comes from a highly flexible loop region, the density for this side chain is good and the distances indicate a very strong interaction. The sugar groups have slightly different positions in the binding sites, which may be favorable in the case of HMP due to the internal hydrogen bond between the hydantoin and the phosphate groups. In the region where the structures of the two ligands differ, most of the contacts with the protein are made in both cases via water molecules. The hydantoin moiety is coplanar with the adenosine group

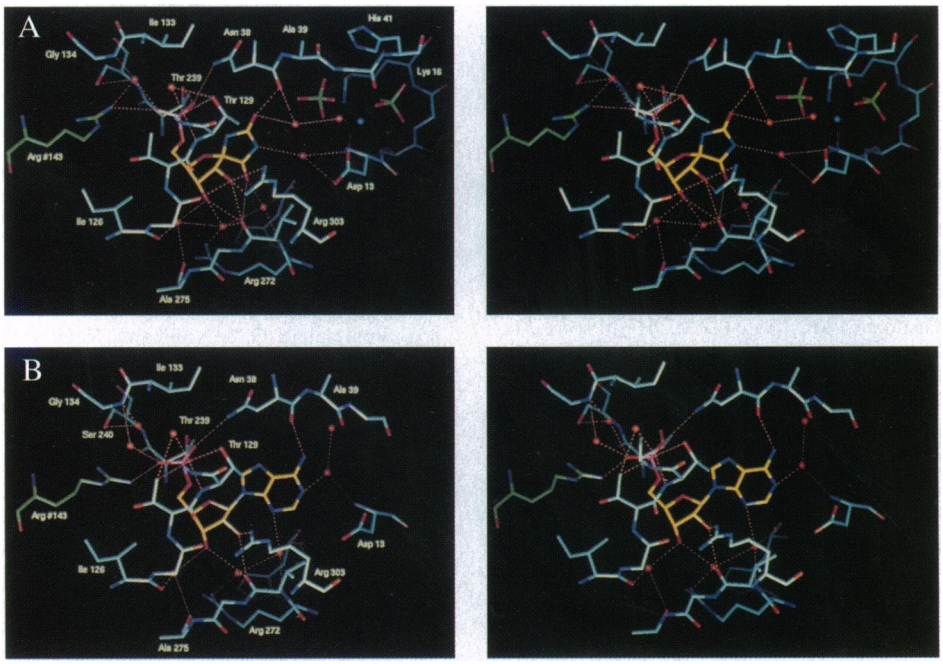


FIG. 5. (*A*) Stereoview of the binding of HMP (yellow) to *E. coli* AdSS. Protein carbon atoms are colored light blue, except for Arg-143 from the other monomer in the dimer, which is green. Water molecules (red spheres) are shown if they are in contact with the inhibitor. All distances between HMP, the protein, and the latter water molecules are shown by orange dashed lines, if they are ≤3.2 Å. Two of the sulfur ions (green) and the sodium ion (blue sphere) are also depicted. (*B*) The binding of AMP to *E. coli* AdSS. See *A* of this figure.

and many of the water molecules lying in the same plane. The two water molecules coordinated to Val-273 are very important for ligand binding and could be considered an intrinsic part of the protein structure, as they are also present in unligated AdSS. All residues in direct or indirect (via water) contact unligated with the inhibitors are completely conserved (Fig. 3).

This binding site is located at one end of a crevice across the middle of the enzyme (Fig. 4*a*). The other end has been proposed (34, 48) to be a binding site for GTP, which has been largely confirmed by site-directed mutagenesis (49). The crystals of AdSS in complex with HMP were obtained in the presence of sulfate ions, and two of the three sulfate ions found in the structure are located in putative phosphate binding sites for GTP (Fig. 5*a*). One of them is bound close to Lys-16, which forms part of the P-loop motif, which in turn binds the γ-phosphate of GTP in $p21^{ras}$ (50). A small sphere of density located between these two sulfates appears to be a sodium ion based on the average bond distances (2.4 Å), octahedral coordination, and the density value itself. This ion is probably located in one of the magnesium binding sites (37), coordinated by Asp-13 and the main chain carbonyl of Gly-40.

The structure of AdSS in complex with HMP represents the first example of a herbicide in complex with its target enzyme. HMP is a natural product and a valuable lead in the search for potent herbicides of novel chemistry. This work has made possible, in the crop protection industry, structure-based design of specific inhibitors of a novel herbicide target based on its protein structure, an approach that has proven to be successful in the pharamaceutical field.

We would like to acknowledge the assistance of E. Baumert, M. Boehler, P. Den Hartog, M. Flaeschel, J. Gaudin, R. Gutekunst, F. Karlin, E. Lanz, C. Logel, S. Potter, C. Schlegel, R. Stoll, and B. Zussy in this work. H.J.F. provided *E. coli* AdSS and R.B.H. provided the unligated AdSS coordinates.

1. Kirkwood, R. C., ed. (1991) *Topics in Applied Chemistry: Target Sites For Herbicide Action* (Plenum, New York).
2. Hock, B., Fedtke, C. & Schmidt, R. R., eds. (1995) in *Herbizid: Metabolismus, Toleranz und Resistenz* (Thieme, Stuttgart), pp. 250–261.
3. Hedin, P. A., Menn, J. J. & Hollingworth, R. M., eds. (1994) *Natural and Engineered Pest Management Agents*, ACS Symposium Series 551 (Am. Chem. Soc., Washington, DC).
4. Sankyo (1987) Eur. Pat. Appl. 0 232 572 A2 (19.08.87).
5. Haruyama, H., Takayama, T., Kinoshita, T., Kondo, M., Nakajima, M. & Haneishi, T. (1991) *J. Chem. Soc. Perkin Trans.* **1,** 1637–1640.
6. Nakajima, M., Itoi, K., Takamatsu, Y., Kinoshita, T., Okasaki, T., Kawakubo, K., Shindou, M., Honma, T., Tohjigamori M. & Haneishi, T. (1991) *J. Antibiot.* **44,** 293–300.
7. Ciba-Geigy (1990) Deutsche Offenlegensschrift 4129-616-A1 (10.9.90).
8. Mitsubishi Kasei (1990) Jpn. Pat. 04222589-A (19.21.90).
9. Nakajima, N., Matsumoto, M., Kirihara, M., Hashimoto, M., Katoh, T. & Terashima, M. (1996) *Tetrahedron* **52,** 1177–1194.
10. Mio, S., Kitagawa, J. & Sugai, S. (1991) *Tetrahedron* **47,** 2133–2144.
11. Mio, S., Ichinose, R., Goto, K. & Sugai, S. (1991) *Tetrahedron* **47,** 2111–2120.
12. Chemla, P. (1993) *Tetrahedron Lett.* **34,** 7391–7394.
13. Harrington, P. M. & Jung, M. M. (1994) *Tetrahedron Lett.* **35,** 5145–5148.
14. Ciba-Geigy (1990) Deutsche Offenlegensschrift 4129-728-A (10.9.90).
15. Burton, J. W., Fairbank, A. J., Choi, S. S., Taylor, H., Watkin, D. J., Winchester, B. G. & Fleet, G. W. J. (1993) *Tetrahedron Lett.* **34,** 6119–6122.
16. Sano H., Mio, S. & Kitagawa, J. (1994) *Tetrahedron Asymmetry* **5,** 2233–2240.
17. Dondoni, A., Scherrmann, M-C., Marra, A. & Delaine, J. (1994) *J. Org. Chem.* **59,** 7517–7520.
18. Bichard, C. J. F., Mitchell, E. P., Wormald, M. R., Watson, K. A., Johnson, L. N., Zographos, S. P., Koutra, D. D., Oikonomakos, N. G. & Fleet, G. W. J. (1995) *Tetrahedron Lett.* **36,** 2145–2148.
19. Brandstetter, T. W., Kim, Y.-H., Son, J. C., Taylor, H. M., Lilley, P. M. Q., Watkin, D. J., Johnson, L. N. & Fleet, G. W. J. (1995) *Tetrahedron Lett.* **36,** 2149–2152.
20. Sano, H., Mio, S., Tsukagachi, N. & Sugai, S. (1995) *Tetrahedron* **51,** 1387–1394.
21. Sano, H. & Sugai, S. (1995) *Tetrahedron* **51,** 4635–4646.
22. Sano, H., Mio, S., Kitagawa, J., Shindou, M., Honma, T. & Sugai, S. (1995) *Tetrahedron* **51,** 12563–12572.
23. Hanessian, S., Sancéau, J.-Y. & Chemla, P. (1995) *Tetrahedron* **51,** 6669–6678.
24. Sano, H., Mio, S., Hamura, M., Kitagawa, J., Shindou, M., Honma, T. & Sugai, S. (1995) *Biosci. Biotech. Biochem.* **59,** 2247–2250.
25. Lamberth, C. & Blarer, S. (1996) *Synth. Commun.* **26,** 75–81.
26. Stayton, M. M., Rudolph, F. B. & Fromm, H. J. (1983) *Curr. Top. Cell. Regul.* **22,** 103–141.
27. Mori, I., Fonné-Pfister, R., Matsunaga, S. I., Tada, S., Kimura, Y., Iwasaki, G., Mano, J. I., Hatano, M., Nakano, T., Koizumi, S. I., Scheidegger, A., Hayakawa, K. & Ohta, D. (1995) *Plant Physiol.* **170,** 719–723.
28. Bass, M. B., Fromm, H. J. & Stayton, M. M. (1987) *Arch. Biochem. Biophys.* **256,** 335–342.
29. Hatch, M. D. (1966) *Biochem. J.* **98,** 198–203.
30. Minet, M., Dufour, M.-E. & Lacroute, F. (1992) *Plant J.* **2,** 417–422.
31. Serra, M. A, Bass, M. B., Fromm, H. J. & Honzatko, R. B. (1988) *J. Mol. Biol.* **200,** 753–754.
32. Rossman, M. G. (1972) *The Molecular Replacement Method* (Gordon and Breach Science, New York).
33. Brunger, A. T. (1992) X-PLOR (Yale Univ. Press, New Haven, CT), Version 3.1.
34. Silva, M. M., Poland, B. W., Hoffman, C. R., Fromm, H. J. & Honzatko, R. B. (1995) *J. Mol. Biol.* **254,** 431–446.
35. Jones, T. A., Zou, J.-Y., Cowan, S. W. & Kjeldgaard, M. (1991) *Acta Crystallogr. A* **47,** 110–119.
36. Laskowski, R. A., McArthur, M. W., Moss, D. S. & Thornton, J. M. (1993) *J. Appl. Crystallogr.* **26,** 282–291.
37. Kang, C. & Fromm, H. J. (1995) *J. Biol. Chem.* **270,** 15539–15544.
38. Spector, T. (1977) *Biochim. Biophys. Acta* **481,** 741–745.
39. Hampton, A., Harper, P. J. & Sasaki, T. (1972) *Biochemistry* **11,** 4965–4969.
40. Hatch, M. D. (1967) *Phytochemistry* **6,** 115–119.
41. Jahngen, E. G. E. & Rossomando, E. F. (1984) *Arch. Biochem. Biophys.* **229,** 145–154.
42. Heim, D. R., Cseke, C., Gerwick, B. C., Murdoch, M. G. & Green, S. B. (1995) *Pestic. Biochem. Phys.* **53,** 138–145.
43. Siehl, D. L., Subramanian, M. V., Walter, E. W., Lee, S.-F., Anderson, R. J. & Toschi, A. G. (1996) *Plant Physiol.* **110,** 753–758.
44. Wolfe, S. A. & Smith, J. M. (1988) *J. Biol. Chem.* **263,** 19147–19153.
45. Von Heime, G. & Nishikawa, K. (1991) *FEBS Lett.* **278,** 1–3.
46. Boland, M-J. & Schubert, K. R. (1983) *Arch. Biochem. Biophys.* **220,** 179–187.
47. Sander, C. & Schneider, R. (1991) *Proteins* **9,** 56–68.
48. Poland, B. W., Silva, M. M., Serra, M. A., Cho, Y., Kim, K. H., Harris, E. M. S. & Honzatko, R. B. (1993) *J. Biol. Chem.* **268,** 25334–25342.
49. Kang, C., Sun, N., Honzatko, R. B. & Fromm, H. J. (1994) *J. Biol. Chem.* **269,** 24046–24049.
50. Pai, E. F., Kabsch, W., Krengel, U., Holmes, K., John, J. & Wittinghofer, A. (1989) *Nature (London)* **341,** 209–214.